INSTITUTE FOR FUSION STUDIES

DOE/ET-53088-477 IFSR #477

Linear Studies of $m = 1$ Modes in High-Temperature Plasmas with a Four-Field Model

A.Y. AYDEMIR
Institute for Fusion Studies
The University of Texas at Austin
Austin, Texas 78712

March 1991

THE UNIVERSITY OF TEXAS

AUSTIN

IFSR #477

Linear Studies of $m = 1$ Modes in High-Temperature Plasmas with a Four-Field Model

A. Y. Aydemir
Institute for Fusion Studies
The University of Texas at Austin
Austin, Texas 78712

The $m = 1$ mode in high temperature plasmas is examined using a simple four-field model of tokamak dynamics derived by Hazeltine, Hsu, and Morrison [Phys. Fluids **30**, 3204 (1987)]. It is shown that, despite its simplicity, the model reproduces with remarkable accuracy results obtained with more sophisticated kinetic treatments in various collisionality regimes. The effects of parallel compressibility on the $m = 1$ mode in the collisional, semi-collisional and collisionless regimes are also discussed. Coupling to the ion sound waves is found to be weakly destabilizing in the collisional regime, and stabilizing in the semi-collisional and collisionless regimes.

I. Introduction

One of the ubiquitous features of tokamak plasmas is the sawtooth oscillations exhibited by the central electron temperature.[1] Since the oscillations affect the central core, the hottest part of the plasma column, and because their understanding and possible control may have significant impact on the present and the next generation of tokamaks, they continue to receive a great deal of attentian, both experimentally and theoretically.

These relaxation oscillations are generally assumed to be intimately connected with the $m = 1$ internal kink mode,[2] which has been studied, in various degrees of detail and sophistication, by many workers in the field. Coppi *et al.*'s unified treatment of the resistive and ideal branches of the mode[3] was later extended to include diamagnetic drift effects.[4] Bussac *et al.*[5] examined geometric effects and found the ideal mode to be stabilized by toroidicity for typical plasma parameters. Subsequent workers considered kinetic effects, finite plasma pressure, and finite ion Larmor radius (FLR) effects.[6–9] More recently, $m = 1$ has been treated with even more sophisticated techniques extending the earlier small-FLR calculations to the arbitrary FLR limit.[10–12]

Our goal in this work is not to add an even more sophisticated model to the already extensive literature on the $m = 1$ mode, but to prepare for a future nonlinear treatment of the $m = 1$ mode that goes beyond the well-known resistive magnetohydrodynamic (MHD) calculations.[13–18] Here we examine the linear properties of a simplified model that describes tokamak dynamics with only four fields: the four-field model of Hazeltine *et al.*,[19] that extends the usual reduced MHD equations by including FLR effects, finite electron and ion drift frequencies, and long-mean-free-path electron dynamics. One goal of the present work is to compare the results of the four-field model in all three collisionality regimes (collisional, semi-collisional, and collisionless $m = 1$ modes) with those results in the literature that have been obtained with more rigorous and complete kinetic treatments. We will see

that the model is eminently successful in this regard, at least for the resistive branch of the $m = 1$ mode (infinite-Δ') that will be considered here. Secondly, we will extend the analysis to include the effects of parallel compressibility, in particular the ion sound waves, on the $m = 1$ mode. A similar analysis for the $m \geq 2$ modes[20] has shown the ion sound waves to be stabilizing. Here we will find that the sound waves are weakly destabilizing in the collisional regime and tend to be stabilizing in the semi-collisional and collisionless regimes. A nonlinear study of the $m = 1$ mode and self-consistent studies of sawtooth oscillations in high-temperature plasmas with this model will be presented in a future publication.

In the next section, the four-field model of Hazeltine *et al.*[19] is described in some detail. In Section III, the linearized version of the model and a resulting general dispersion equation are presented. In Sect. IV, the dispersion relation without the ion-sound modifications are compared with those in the literature, and the effects of ion sound waves in collisional, semi-collisional, and collisionless regimes are discussed. Finally, a discussion of the results and conclusions are presented in Section V.

II. The Four-Field Model

The four-field model used in this study is a simplified nonlinear description of tokamak dynamics that extends widely used reduced resistive magnetohydrodynamic (MHD) models into high temperature regimes by including electron and ion diamagnetic drifts, finite-ion-Larmor-radius (FLR) effects, and long-mean-free-path electron dynamics in a self-consistent manner.[19]

Omitting the curvature terms and some other terms of order $\rho_i^2 \nabla_\perp^2$, and including terms due to finite electron inertia in the Ohm's law, we write the four-field model of Hazeltine *et al.*[19] in the form

$$\frac{\partial U}{\partial t} + [\phi, U] + \nabla_{\|} J = \delta\tau \nabla_{\perp} \cdot [p, \nabla_{\perp}\phi], \tag{1}$$

$$\frac{\partial \psi}{\partial t} + \nabla_{\|} [\phi - (1+\tau)\delta p] = \eta J + \delta_s^2 \left\{ \frac{\partial J}{\partial t} + [\phi - \delta\tau p, J] \right\}, \tag{2}$$

$$\frac{\partial p}{\partial t} + [\phi, p] + \beta \nabla_{\|} [v + 2\delta J] = 0 \tag{3}$$

$$\frac{\partial v}{\partial t} + \frac{1}{2}(1+\tau)\nabla_{\|} p + [\phi - \delta\tau p, v] = 0, \tag{4}$$

$$\phi = \phi_{elect} + \delta\tau p, \tag{5}$$

$$J = \nabla_{\perp}^2 \psi, \quad U = \nabla_{\perp}^2 \phi, \quad \tau = T_i/T_e, \tag{6}$$

$$\beta = \frac{nkT_e}{B_T^2/2\mu_o} \quad \delta = \frac{c/2\omega_{pi}}{a}, \quad \delta_s = \frac{c/\omega_{pe}}{a} = 2\left(\frac{m_e}{m_i}\right)^{1/2} \delta. \tag{7}$$

The variables have been normalized as follows: $t \rightarrow t/\tau_{Hp}, \mathbf{r} \rightarrow \mathbf{r}/a, \eta = \tau_{Hp}/\tau_R$, where $\tau_{Hp} = a/u_{Hp}$, $\tau_R = \mu_o a^2/\eta_o$, and $u_{Hp} = B_{po}^2/\sqrt{\rho_o \mu_o}$. τ_{Hp} and τ_R are the poloidal Alfvén time and the resistive diffusion time, respectively, defined in terms of the minor radius a, a characteristic poloidal field strength B_{po}, and resistivity η_o.

The brackets are defined by $[\phi, U] = \hat{\zeta} \cdot \nabla_{\perp}\phi \times \nabla_{\perp} U$, where $\hat{\zeta}$ is a unit vector in the toroidal direction, and $\nabla_{\perp}$ is the 2-D gradient in the plane perpendicular to the magnetic field. The parallel gradient operator is defined as $\nabla_{\|} J = \partial J/\partial\zeta + [J, \psi]$ for any scalar J. The parameter δ, in combination with the electron β, is related to the ion Larmor radius, as it can be shown that

$$\tau\delta^2\beta = (\rho_i/2)^2, \tag{8}$$

where ρ_i is the ion gyro radius normalized to the minor radius. Finally, δ_s is the collisionless skin depth.

The vorticity equation, Eq. (1), includes a term due to ion gyroviscosity on the right hand side, through which the ion diamagnetic drift frequency is introduced in the linear regime. The parallel Ohm's law, Eq. (2), includes the parallel pressure gradient, which introduces the electron diamagnetic drift frequency, and electron inertia terms, which bring the collisionless skin-depth length-scale and the associated collisionless physics into the system. An isothermal equation of state is assumed; thus, the equation for pressure, Eq. (3), actually describes the electron density. The parallel electron compressibility appearing in this equation makes it possible to describe long-mean-free-path (semi-collisional) physics. Finally, v is the parallel ion velocity through which parallel sound speed physics is introduced. Note that the stream function ϕ is equal to the electrostatic potential ϕ_{elect} only in the cold ion limit, $\tau = 0$.

The frequency $\omega_{pe(i)}$ is the electron (ion) plasma frequency, and the drift frequencies that we will encounter later are defined by

$$\omega_{*e} = -\delta \frac{m}{r} p_0', \qquad \omega_{*i} = -\tau \omega_{*e}, \tag{9}$$

where m is the poloidal mode number, and $p_0'(r)$ is the local equilibrium density gradient.

The apparent simplicity of the model makes it particularly useful in nonlinear computational studies; however, the present work will focus on various linear modes that are described by the model and is intended to serve as an introduction to nonlinear computional studies that will follow at a later date. Below we will briefly describe the linearized equations obtained from Eqs. (1-4). In subsequent sections, dispersion relations for $m = 1$ modes in various collisionality regimes will be derived and discussed.

III. Linear Equations

Linearizing Eqs. (1-4) and ignoring gradients of the equilibrium quantities U_o and J_o, we obtain in the slab limit

$$\frac{d^2\phi}{dx^2} - \frac{x}{x_A}\frac{d^2\psi}{dx^2} = 0, \tag{10}$$

$$\psi - \frac{x}{x_A \Delta_i}\phi = i\widehat{x_{\eta_s}}^2 \ \frac{d^2\psi}{dx^2}, \tag{11}$$

where we assumed the perturbed quantities have the form $f(r,\theta,\zeta) = f(r)\exp[i(-\omega t + m\theta - n\zeta)]$. The variable x measures the distance from the rational surface, $x = r - r_s$, and we have used for the parallel wave-vector $k_\| = -\{n + (m/r)(\partial\psi_o/\partial r)\} = k'_\| x$.

Various length scales used throughout this work are defined below:

$$x_A = \frac{\omega}{k'_\|}, \quad x_{A*} = \frac{\omega\Delta_i^{1/2}}{k'_\|}, \quad x_s = \frac{x_A}{c_s}, \tag{12}$$

$$x_\eta^2 = \frac{\eta_\|}{\omega}, \quad x_{\eta_s}^2 = x_\eta^2 - i\delta_s^2, \tag{13}$$

$$x_J^2 = \Delta_i \frac{i x_{\eta_s}^2 x_s^2}{4\delta^2 + i x_{\eta_s}^2} = \frac{i x_{\eta_s}^2 x_{A*}^2}{(4\delta^2 + i x_{\eta_s}^2)c_s^2}, \tag{14}$$

$$i\widehat{x_{\eta_s}}^2 = \left(\frac{i x_{\eta_s}^2}{\Delta_e}\right) \ \frac{1 - x^2/x_J^2}{1 - x^2/(\Delta_e x_s^2)}, \tag{15}$$

$$\text{where} \quad \Delta_e = 1 - \frac{\omega_{*e}}{\omega}, \quad \Delta_i = 1 - \frac{\omega_{*i}}{\omega}, \quad \text{and} \quad c_s^2 = \frac{1+\tau}{2}\beta. \tag{16}$$

Above, x_{A*} is the inertial layer width, x_s is the sound layer width, and x_{η_s} is the resistive layer width, defined in terms of η_s, which includes the finite-electron-inertia modifications of the parallel Spitzer resistivity but no other physics. Essentially all the non-MHD physics of the four-field model is contained in the generalized resistive layer width, $\widehat{x_{\eta_s}}$, defined in Eq. (15). The quantity x_J is a measure of the current channel width; its meaning will become

more transparent during the discussion of the semi-collisional regime below. Note that for convenience we have absorbed a factor of $(1+\tau)$ into the definition of the ion sound speed c_s; the actual ion sound speed in the four-field model is equal to $\sqrt{\beta/2}$.

Equations (10) and (11) can be combined to yield[3,21]

$$\frac{d}{dx}\left[\frac{i\widehat{x\eta_s}^2}{x^2}\frac{dE}{dx}\right]-\left[\frac{1}{x^2}-\frac{1}{x_{A*}^2}\right]E=0, \tag{17}$$

where we defined $E=\phi'$, which measures the radial electric field. This dispersion equation needs to be solved with the boundary condition $E\to 0$ for $|x|\to\infty$. Note that in general, Eqs. (10) and (11) lead to an inhomogeneous version of the Eq. (17); however, the inhomogeneity can be shown to vanish in the limit that the ideal internal kink mode becomes marginally stable ($\Delta'\to\infty$).[3,21] Thus, this work will be mainly concerned with the "resistive" branch of the $m=1$ mode. This is not an overly restrictive assumption because many of the interesting results are obtained in this limit.

Below we will examine the solutions of Eq. (17) in various collisionality regimes. Our aim will be two-fold. We will focus on the effects of ion sound waves on the $m=1$ mode, while at the same time making connections with previously published results, some obtained using sophisticated kinetic treatments, thus exhibiting the versatility of the four-field model. An important result of this analysis will be that the sound waves are destabilizing for $m=1$ in the collisional regime, contrary to the results obtained for $m\geq 2$ (finite-Δ') modes,[20] but have a stabilizing influence in the semi-collisional and collisionless regimes.

IV. Effects of Ion Sound Waves

Before entering a discussion of the effects of parallel compressibility on the $m=1$ mode, we need to make explicit what is meant by collisional, semi-collisional, and collisionless regimes in the context of the four field model.

In the definitions of various length-scales in Eqs. (12-15), the FLR parameter δ explicitly

appears only in Eq. (14), and in the form $4\delta^2 + ix_{\eta_s}^2$. Thus, for $|x_{\eta_s}| \gg 2\delta$, FLR effects become unimportant. Note, however, that finite drift frequencies and sound speed are still retained in this limit, giving rise to a "collisional drift-tearing" regime. The opposite limit $2\delta \gg |x_{\eta_s}|$ describes semi-collisional, or collisionless regimes, and the boundary between these two regimes is determined by $|x_\eta| \sim \delta_s$, as it can be seen in Eq. (13). Using $\eta_\parallel = m_e\nu_{ei}/2e^2n_e$, where ν_{ei} is the electron-ion collision frequency, these results can be summarized as follows:

$$|x_{\eta_s}| \sim |x_\eta| > 2\delta, \quad \left(\frac{\nu_{ei}}{\omega} > 2\frac{m_i}{m_e}\right) \quad \text{collisional regime,} \tag{18}$$

$$|x_{\eta_s}| \sim |x_\eta| < 2\delta, \quad \left(1 < \frac{\nu_{ei}}{\omega} < 2\frac{m_i}{m_e}\right) \quad \text{semi-collisional regime,} \tag{19}$$

$$|x_{\eta_s}| \sim \delta_s \quad (x_\eta < \delta_s), \quad \left(\frac{\nu_{ei}}{\omega} < 1\right) \quad \text{collisionless regime.} \tag{20}$$

We begin with the discussion of the effects of sound waves in the collisional regime.

A. Collisional Regime

In the collisional regime, $|x_{\eta_s}| > 2\delta$, or $\nu_{ei}/\omega > 2m_i/m_e$, we have $x_J^2 \simeq \Delta_i x_s^2$, and $\widehat{x_{\eta_s}}$ reduces to

$$i\widehat{x_{\eta_s}}^2 \simeq \left(\frac{ix_\eta^2}{\Delta_i}\right)\frac{x^2 - \Delta_i x_s^2}{x^2 - \Delta_e x_s^2}. \tag{21}$$

With this form of the generalized resistivity ($i\widehat{x_{\eta_s}}^2 = i\eta_*/\omega$, where η_* is the generalized resistivity), the dispersion equation (17) can be solved in terms of the variational functional[22]

$$H = \int_{-\infty}^{\infty}\left\{\left(\frac{ix_\eta^2}{\Delta_i}\right)\left(\frac{x^2 - \Delta_i x_s^2}{x^2 - \Delta_e x_s^2}\right)\left(\frac{E'^2}{x^2}\right) + \left(\frac{1}{x^2} - \frac{1}{x_{A*}^2}\right)E^2\right\}dx. \tag{22}$$

Assuming a trial function of the form $E = \exp(-\alpha x^2/2)$, the integrals in Eq. (22) are easily performed to yield

$$H = \pi^{1/2}\left\{-\left[2\alpha^{1/2} + \frac{\alpha^{-1/2}}{x_{A*}^2}\right] + \frac{ix_\eta^2}{\Delta_i}\alpha^{3/2}\left[\left(1 - \frac{\Delta_i}{\Delta_e}\right)\zeta Z(\zeta) + 1\right]\right\}, \tag{23}$$

where $\zeta = \alpha^{1/2}\Delta_e^{1/2}x_s$, α is a parameter to be determined variationally, and $Z(\zeta)$ is the plasma dispersion function. For bounded solutions, we require $\mathrm{Re}(\alpha) > 0$. The parameter α

and the dispersion relation are determined by the equations $H = 0$ and $\delta H = 0$ ($\partial H/\partial\alpha = 0$), which after some algebra lead to

$$\alpha^2 = -\frac{\Delta_e}{ix_\eta^2 x_{A*}^2} + \mathcal{O}(c_s^4), \tag{24}$$

$$\alpha = \frac{\Delta_e}{ix_\eta^2} + \frac{1}{4}\left(1 - \frac{\Delta_i}{\Delta_e}\right)\frac{c_s^2}{x_{A*}^2}. \tag{25}$$

Above we have assumed that the mode width $w \sim \alpha^{-1/2} \ll \Delta_e^{1/2} x_s$ and used the large-argument expansion for the Z function, with the further assumption that $|\mathrm{Im}(\zeta)| > |\mathrm{Re}(\zeta)|$. Equation (24) reveals that the mode width is not affected, to order $c_s^2 \sim \beta$, by finite$-\beta$ effects. Combining equations (24) and (25) leads to the dispersion relation

$$\omega(\omega - \omega_{*e})(\omega - \omega_{*i}) = -i\gamma_R^3\left\{1 + \frac{1}{2}\left(1 - \frac{\Delta_i}{\Delta_e}\right)c_s^2\right\}, \tag{26}$$

where $\gamma_R = k_\parallel'^{2/3}\eta^{1/3}$ is the growth rate of the classical, resistive $m = 1$ kink mode, and we recall that $\Delta_e = 1 - \omega_{*e}/\omega$, and $\Delta_i = 1 - \omega_{*i}/\omega$. Note that for $c_s = 0$, we obtain the well-known dispersion relation of Ara, Basu *et al.*[4]

Equation (26) was derived with the following assumptions: i) $\mathrm{Re}(\alpha) > 0$, which localizes the mode around the rational surface. This requirement is easily satisfied by unstable modes. ii) $\mathrm{Im}(\zeta) > 0$ and $|\mathrm{Im}(\zeta)| > |\mathrm{Re}(\zeta)|$, which were used in the derivation of the terms involving $Z-$functions and their asymptotic expansions. Numerical solution of Eq. (26) shows two unstable branches, one with an approximately zero real-frequency and $\gamma \simeq \gamma_R$, and a second one with a real frequency $\omega_r \simeq \omega_{*e}$, and $\gamma \ll \omega_{*e}$. Although both of these branches satisfy the consistency requirement $\mathrm{Re}(\alpha) > 0$, the second branch with $\omega \simeq \omega_{*e}$ is inconsistent with the second set of assumptions and is not considered any further.

For $\omega_{*(e,i)} \ll \gamma_R$, Eq. (26) can be solved perturbatively to give

$$\omega = \left\{\frac{\omega_{*e} + \omega_{*i}}{3} - (\omega_{*e} - \omega_{*i})\frac{c_s^2}{6}\right\} + i\gamma_R\left\{1 - \frac{\omega_{*e}^2 - \omega_{*e}\omega_{*i} + \omega_{*i}^2}{9\gamma_R^2} + \frac{2\omega_{*e}^2 - 3\omega_{*e}\omega_{*i} + \omega_{*i}^2}{18\gamma_R^2}c_s^2\right\}. \tag{27}$$

Thus, we find that coupling to the ion sound terms is destabilizing for the resistive $m = 1$ mode in the collisional regime, although the effect is weak and appears only in the second order in $\omega_{*(e,i)}/\gamma_R$. In contrast, the sound terms were found to be stabilizing for the $m = 2$ modes.[20] In Fig. 1, predictions of Eq. (27) are compared with the results of an eigenvalue code that integrates the linearized versions of Eqs. (1-4) [not Eq. (17), which was derived from those equations]. In Fig. 1(a), the mode frequency, normalized to γ_R, is plotted as a function of $\beta = c_s^2$ (we assume $\tau = 1$) for $\eta = 10^{-8}$, $\gamma_R/\omega_{*e} = 10$, and a q–profile with $q_o = 0.90$, and $q_l = 3.5$ ($k'_{||} = -1.87$). In this and subsequent plots, β is varied while keeping $\omega_{*(e,i)}$ fixed. Note that the sound terms break the symmetry between the electron and ion drift frequencies; with $c_s^2 > 0$, the mode rotates in the ion direction with a frequency that increases with c_s^2, $\omega_r \simeq \omega_{*i} c_s^2$. Figure 1(b) shows the change in the growth rate as function of β under the same conditions, clearly indicating the destabilizing effect of the ion sound waves. For comparison, for the parameters used above, Eq. (27) predicts $\omega_r/\gamma_R = -3.33 \times 10^{-2}\beta$, and $(\gamma - \gamma_R)/\gamma_R = 3.33 \times 10^{-3}(-1 + \beta)$. Thus, the variational solution for ω_r and γ is found to be approximately within 20% of the numerical solutions.

Although a variational analysis of the collisional problem under assumptions consistent with $\omega_r \simeq \omega_*, \gamma_R/\omega_{*e} \ll 1$ is possible, a search with our eigenvalue code has revealed no unstable modes in this parameter regime. Earlier, we had found a mode driven by the gradient of the drift frequency[23] with $\omega_r \simeq \omega_{*e}$. However, the ion sound terms were found to be strongly stabilizing for this mode, and the effects of finite ω'_* are not considered here. Therefore, we next turn our attention to the more interesting semi-collisional regime.

B. Semi-Collisional Regime

In this regime, defined by Eq. (19), collisions are still important ($\nu_{ei}/\omega > 1$); however, now the electron mean-free-path is long enough for the parallel electron compressibility to play a significant role in limiting the width of the current channel to far below the mode

width itself.[7–9,22,24] The length-scale x_J is now given by $x_J^2 = ix_{\eta_s}^2 x_{A*}^2/(4\delta^2 c_s^2) \ll (x_{A*}^2, x_s^2)$. For $x^2 > x_J^2$, the effective resistivity (or "ac" resistivity) is greatly increased, thus confining the current to $|x| < x_J$, a region much narrower than observed in the collisional regime, where the current channel width (and the mode width) is given by $w_c = (-ix_\eta^2 x_{A*}^2/\Delta_e)^{1/4}$ [See Eq. (24)]. At the same time, the parallel electric field is less effectively shorted out by the electrons for $|x| > x_J$, leading to a much wider region around the rational surface with significant parallel electric fields. A stronger coupling to the ion sound waves, caused by the increased mode width, makes the ion-sound effects more important than was observed in the collisional case.

A variational solution of the dispersion equation, Eq. (17), in the semi-collisional regime proves unfeasible because of the presence of three distinct length-scales. Although it is well known that an accurate trial function is not necessary for an accurate variational evaluation of the eigenvalues,[22] here the trial functions amenable to analytic treatment do not lead to accurate dispersion relations that agree with numerical solutions of the linear equations. Thus, we are forced to use a boundary-layer analysis with three sub-layers across which the solutions have to be asymptotically matched. These three layers are defined by 1) $x \lesssim x_J$, 2) $x \lesssim x_{A*}$, and 3) $x \lesssim x_s$. Finally, the solution from sub-layer 3 has to be asymptotically matched to the exterior solution (the "ideal solution" from $x > x_s$), which simply requires decaying solutions for large x in layer 3.

It is more convenient to carry out the analysis in terms of a new variable, $F = E_{||}/x$, where we define $E_{||} = \psi - (x/x_A\Delta_i)\phi$ [See Eq. (11)]. In terms of F, Eq. (17) becomes[9]

$$\frac{d}{dx}\left[\frac{x^2}{x^2 - x_{A*}^2}\right]\frac{dF}{dx} - \frac{x^2}{w_c^4}\left[\frac{1 - x^2/\Delta_e x_s^2}{1 - x^2/x_J^2}\right]F = 0, \tag{28}$$

where w_c is the "classical" mode width, $w_c^4 = (-ix_{\eta_s}^2 x_{A*}^2/\Delta_e)$. Note that in the semi-collisional regime, we have $x_{\eta_s}^2 = x_\eta^2 - i\delta_s^2 \simeq x_\eta^2$. However, to maintain generality and applicability of the results to the collisionless regime, we will continue to use $x_{\eta_s}^2$ in this section for the square of the resistive diffusion length scale.

1) In layer 1 ($x \lesssim x_J$), Eq. (28) reduces to

$$\frac{d}{dx}x^2\frac{dF}{dx} - \frac{\Delta_e}{ix_{\eta_s}^2}\left[\frac{x^2}{1-x^2/x_J^2}\right]F = 0. \tag{29}$$

The odd solution ($E_{||}$ is assumed to be even), written in terms of Legendre functions, is

$$H(x) = P_\nu(x/x_J) - P_\nu(-x/x_J), \tag{30}$$

where $H = d(xF)/dx$, and

$$\nu(\nu+1) = -\frac{\Delta_e x_J^2}{ix_{\eta_s}^2} \simeq -\frac{\Delta_e x_{A*}^2}{4\delta^2 c_s^2}. \tag{31}$$

Large-argument expansion of H gives

$$F_1(x) \approx x^\nu - \left(\frac{\nu+1}{\nu}\right)\left(\frac{x_J}{2}\right)^{2\nu+1}\cot(\frac{\pi}{2}\nu)\left(ie^{-i\pi\nu}\right)\frac{\Gamma(-1/2-\nu)\Gamma(1+\nu)}{\Gamma(1/2+\nu)\Gamma(-\nu)}x^{-(\nu+1)} \tag{32}$$

2) In layer 2, $x_J \ll x \lesssim x_{A*}$, Eq. (28) becomes

$$\frac{d}{dx}\frac{x^2}{x^2-x_{A*}^2}\frac{dF}{dx} - \frac{\Delta_e}{4\delta^2 c_s^2}F = 0. \tag{33}$$

The solution can be written in terms of modified Bessel functions,

$$u(\zeta) = I_\mu(\zeta) + AK_\mu(\zeta), \tag{34}$$

where A is a constant to be determined, $\zeta = (\Delta_e^{1/2}/2\delta c_s)x$, and μ is given by

$$\mu^2 = \frac{1}{4} - \frac{\Delta_e x_{A*}^2}{4\delta^2 c_s^2}. \tag{35}$$

$u(\zeta)$ is related to $F(x)$ through

$$f_2(x) = x^{1/2}u(\zeta),$$
$$\frac{dF_2}{dx} = \frac{x^2-x_{A*}^2}{x^2}f_2(x).$$

Small-argument expansion of $u(\zeta)$ leads to

$$f_2(x) \approx x^{\mu+1/2} + \frac{A}{2}\Gamma(\mu)\Gamma(\mu+1)\left[\frac{\Delta_e^{1/2}}{4\delta c_s}\right]^{-2\mu}x^{-\mu+1/2}, \tag{36}$$

where we assumed $\mathrm{Re}(\mu) > 0$. Using $dF_2/dx \approx -(x_{A*}^2/x^2) f_2(x)$ to obtain $F_2(x)$ and matching the result with $F_1(x)$ from Eq. (32) determines the constant A,

$$A = -2\left(\frac{\mu+1/2}{\mu-1/2}\right)^2 \left[\frac{-ix_J\Delta_e^{1/2}}{8\delta c_s}\right]^{2\mu} \frac{\Gamma(-\mu)\Gamma(\mu+1/2)}{\Gamma^2(\mu)\Gamma(-\mu+1/2)\Gamma(\mu+1)} \cot\frac{\pi}{2}(\mu-1/2), \qquad (37)$$

where we also noted that matching requires $\nu = \mu - 1/2$, which is identically satisfied.

A large-argument expansion of $u(\zeta)$ is not needed. Using (8) and (16) we can show that $\delta^2 c_s^2 = (\rho_i/2)^2(T_e/T_i+1)/2$, which leads to

$$\zeta = \frac{\Delta_e^{1/2}}{2\delta c_s} x = \left[\frac{2\Delta_e}{T_e/T_i+1}\right]^{1/2} \left(\frac{x}{\rho_i}\right). \qquad (38)$$

Thus, for $x \simeq x_{A*}$, we have $\zeta \simeq x_{A*}/\rho_i$. We assume $x_{A*}/\rho_i < 1$ in the semi-collisional regime and use (36) for $x \sim x_{A*}$ (large-argument limit) also. Note that this assumption, which also implies $\mu \simeq 1/2$, needs to be justified *a posteriori.*

3) In layer 3, $x_{A*} \ll x \lesssim x_s$, Eq. (28) simplifies to

$$\frac{d^2F}{dx^2} - \frac{\Delta_e x_J^2}{i x_{\eta_s}^2 x_{A*}^2}\left[1 - \frac{x^2}{\Delta_e x_s^2}\right] F = 0. \qquad (39)$$

The solution that decays for $x \to \infty$ is given in terms of parabolic cylinder functions,[25] $F_3(z) = U(a,z)$, where

$$a = \frac{i\Delta_e x_s}{4\delta c_s}, \qquad (40)$$

$$z = x/\bar{x}, \quad \bar{x} = \left(-\delta^2 c_s^2 x_s^2\right)^{1/4} = \left(-\delta^2 x_A^2\right)^{1/4}. \qquad (41)$$

Expanding $U(a,z)$ for $z \to 0$ and using $f_3(x) = x^2/(x^2 - x_{A*}^2)(dF_3/dx) \approx dF_3/dx$, we obtain

$$f_3(x) \approx x - 2^{1/2}\frac{\bar{x}}{a}\frac{\Gamma(a/2+3/4)}{\Gamma(a/2+1/4)}. \qquad (42)$$

This function can match the $f_2(x)$ of Eq. (36) only if $\mu \simeq 1/2$; we will show presently that the $\mu \to 1/2$ limit, requiring $x_{A*} < \rho_i$, is self-consistent. Thus, Eqs. (36) and (42) yield the dispersion relation

$$2^{1/2}\frac{(1/2-\mu)}{(1/2+\mu)^2}\frac{\Gamma(3/2-\mu)\Gamma(1+\mu)}{\Gamma(1/2+\mu)\Gamma(1-\mu)}\tan\frac{\pi}{2}(\frac{1}{2}-\mu)=-\left[i\frac{ax_J}{2\bar{x}}\right]\frac{\Gamma(1/4+a/2)}{\Gamma(3/4+a/2)} \tag{43}$$

Expanding the left-hand-side around $\mu = 1/2$, (43) can be put in the form

$$\frac{\Delta_e^{3/2}\Delta_i^{3/2}x_A^3}{x_{\eta_s}} = \frac{8}{\pi}\, i^{7/2}\, \delta^2 c_s^2 G(a), \tag{44}$$

where

$$G(a) = \left(\frac{a}{2}\right)^{1/2}\frac{\Gamma(1/4+a/2)}{\Gamma(3/4+a/2)}. \tag{45}$$

We can easily recover from (44) the semi-collisional dispersion relation for $m = 1$ without the sound effects. From the definition of a above, we have $a \simeq x_s/4\delta c_s \simeq x_s/2\rho_i$. Thus, if we ignore the ion sound contributions to the dispersion relation by letting $x_s \to \infty$ at fixed ρ_i, we have $G(a) \to 1$ and(44) reduces to

$$\omega(\omega-\omega_{*e})^3(\omega-\omega_{*i})^3 = \left(\frac{8}{\pi}\right)^2\, i^7\, \delta^4 c_s^4 k_{||}'^6 \eta, \tag{46}$$

A perturbative solution of (46) for $\omega \sim i\gamma \gg \omega_*$ gives

$$\omega = \frac{3(\omega_{*e}+\omega_{*i})}{7} + i\gamma_{sc}, \tag{47}$$

where the semi-collisional growth-rate is given by

$$\gamma_{sc} = \left(\frac{8}{\pi}\right)^{2/7}\delta^{4/7}c_s^{4/7}k_{||}'^{6/7}\eta^{1/7}. \tag{48}$$

Note that (46) appears to be exactly equivalent to the dispersion relation found by Hahm.[26] Hahm uses a kinetic approach, starting with the drift-kinetic equation for the electron response and the gyro-kinetic equation for the ion response. In addition, in the resistive layer, which is less than one ion gyro-radius wide in the semi-collisional regime, ions are treated as unmagnetized. In fact, slight differences between Hahm's dispersion relation and Drake *et al.*'s earlier work[7,8] are attributed to this more physical treatment of the ion response. Thus, the fact that we obtained the same dispersion relation as Hahm's

from a simplified two-fluid model is quite remarkable and indicates that the four field model, despite its simplicity, contains essential features of the sophisticated kinetic treatments. More supportive evidence in this direction will be presented in the discussion of the collisionless regime. Parenthetically, we have also reproduced Hahm and Chen's dispersion relation for the semi-collisional kinetic Alfvén waves[27] with the four-field model; however, a discussion of this mode is outside the scope of this paper.

In order to consider the effects of ion sound waves in the semi-collisional regime, we note that $a \simeq x_s/(2\rho_i)$ and asymptotically expand $G(a)$ for large a to obtain $G(a) \approx 1 - 1/(4a^2)$. Substituting for $G(a)$ in (44) then leads to the ion-sound-modified dispersion relation

$$\omega(\omega - \omega_{*e})^3(\omega - \omega_{*i})^3 = (i\gamma_{sc})^7 \left\{1 + \left(\frac{\rho_i}{2}\right)^2 \left(\frac{T_e}{T_i} + 1\right) \frac{c_s^2 k_\parallel'^2}{(\omega - \omega_{*e})^2}\right\}, \tag{49}$$

where we used $\delta^2 c_s^2 = \rho_i^2(T_e/T_i + 1)/8$. Finally, assuming $\omega \sim i\gamma_{sc} \gg \omega_*$ and solving (49) perturbatively leads to

$$\omega = \frac{3(\omega_{*e} + \omega_{*i})}{7} + i\gamma_{sc}\left\{1 - \frac{1}{28}\left(\frac{T_e}{T_i} + 1\right)\rho_i^2 \frac{c_s^2 k_\parallel'^2}{\gamma_{sc}^2}\right\}. \tag{50}$$

Note that the ion-sound waves have a stabilizing influence in the semi-collisional regime, contrary to what was observed in the collisional regime above, although the effect is again rather weak.

The semi-collisional dispersion relation (49) was obtained in the limit $a \sim x_s/\rho_i \gg 1$. In the opposite limit, $a \ll 1$, we obtain

$$\omega(\omega - \omega_{*e})^2(\omega - \omega_{*i})^3 = i^6 \frac{8}{\pi^2}\left[\frac{\Gamma(1/4)}{\Gamma(3/4)}\right]^2 \delta^3 c_s^2 k_\parallel'^5 \eta, \tag{51}$$

which predicts a mode with a stronger dependence on η, $\gamma \sim \eta^{1/6}$. However, $a \ll 1$ seems to be an unphysical limit, requiring very high β; it will not be considered further.

In Figures (2-4), analytic results of this section are compared with numerical calculations using an eigenvalue code that solves the linearized versions of the original four-field equations (1-4). Fig. 2 shows the scaling of the growth rate (ion-sound-modified) with η for

$\tau = 1$, $\gamma_{sc}/\omega_* \simeq 10$, $\delta = 2.0 \times 10^{-2}$, $\beta = 1.0 \times 10^{-2}$, which gives for the ion Larmor radius $\rho_i = 4.0 \times 10^{-3}$. Recall that all lengths are normalized to the minor radius. The observed scaling, $\gamma \sim \eta^{0.164}$, is within 15% of the theoretically expected value of $\gamma \sim \eta^{1/7}$. Fig. 3 shows the relative change in the growth rate as a function of $\beta = c_s^2$ ($\tau = 1$ is assumed) while maintaining $\rho_i = 4 \times 10^{-3}$. The stabilizing influence of the ion sound waves is clearly demonstrated. The numerically observed slope of -0.383 is within 12% of the theoretically expected value of $-(\rho_i^2/14)(k_\parallel'^2/\gamma_{sc}^2) = -0.435$, where we used $k_\parallel' = -1.87$ and $\gamma_{sc} = 3.03 \times 10^{-3}$. Fig. 4 shows the typical eigenfunctions in the semi-collisional regime. For comparison, both $J_\parallel$ (Fig. 4(a)) and $\mathcal{E}_\parallel \equiv \psi - (x/x_A \Delta_i)\phi_{elect}$ (Fig. 4(b)) are plotted. The figures show a region centered around the rational surface, indicated with r_s, with a width of 5% of the minor radius. Approximate locations of $r_s + x_{A*}$, $r_s + \rho_i$, and $r_s + x_s$ are also shown in Fig. 4(b). It is clear that the current channel is localized within $|r - r_s| \lesssim x_J$ ($x_J \simeq 2.3 \times 10^{-4}$ here), while $\mathcal{E}_\parallel$ extends over a much wider region. Note also that $\mathcal{E}_\parallel$ exhibits variations on length scales x_J, ρ_i, and x_s, which, as it was indicated earlier, makes a variational treatment of the problem quite difficult.

In the derivation of the dispersion relations above, we assumed that the Alfvén layer width is less than the ion Larmor radius, $x_{A*} < \rho_i$. Zhang[28] has pointed out that this inequality will hold for modes with $\omega \simeq \omega_{*i}$. However, for the modes under consideration here with $\omega \sim \gamma_{sc} \gg \omega_*$, we have to provide an *a posteriori* justification. Using $\gamma \simeq \gamma_{sc}$, we can show that

$$\left(\frac{x_{A*}}{\rho_i}\right)^7 \simeq \frac{1}{2\pi^2} \frac{\eta}{(\delta c_s)^3 k_\parallel'}. \tag{52}$$

Thus, $x_{A*}/\rho_i < 1$ for

$$\eta < \left(\frac{\pi}{2}\right)^2 k_\parallel' \rho_i^3, \tag{53}$$

which seems to hold for all large tokamaks. For reference, we list below values of various

length scales for $\eta = 1.0 \times 10^{-9}$, $\beta = 1.0 \times 10^{-2}, \delta = 2.0 \times 10^{-2}$:

$$\gamma = 3.02 \times 10^{-3}, \quad k'_{\|} = -1.87,$$
$$x_J \simeq 2.33 \times 10^{-4}, \quad x_{\eta_s} \simeq 5.75 \times 10^{-4},$$
$$x_{A*} \simeq 1.62 \times 10^{-3}, \quad x_s \simeq 1.62 \times 10^{-2},$$
$$w_c \simeq (x_{\eta_s} x_{A*})^{1/2} \simeq 9.65 \times 10^{-4}, \quad \rho_i = 4.0 \times 10^{-3}.$$

Although we have $x_{A*} < \rho_i$, it is clear that x_{A*} is not much less than ρ_i. Therefore, the accuracy of the matching analysis is somewhat surprising. It should probably be attributed to the fact that lowest order terms in the expansion of the left-hand-side of (43) are second order in $(\mu - 1/2)$, thus fourth order in (x_{A*}/ρ_i).

C. Collisionless Regime

For $\nu_{ei}/\omega < 1$, we can obtain a dispersion relation for a collisionless $m = 1$ mode using the results of the previous sections on collisional or semi-collisional modes. Starting with the collisional results in Eqs. (24) and (25), and ignoring diamagnetic and sound effects by letting $\Delta_e \to 1$, $x_{A*} \to x_A$, and $c_s \to 0$, we obtain the well-known dispersion relation for the resistive $m = 1$ mode[3]

$$x_A^2 = -i x_\eta^2, \tag{54}$$

which immediately leads to the purely growing mode $\gamma_R = k'^{2/3}_{\|} \eta^{1/3}$. If we now assume $\nu_{ei}/\omega < 1$, we can replace x_η^2 by $-i\delta_s^2$ in Eq. (54) to obtain a dispersion relation for a purely growing "inertial mode"[6,29]

$$\gamma = k'_{\|} \delta_s, \tag{55}$$

where δ_s is the collisionless skin depth. However, in the context of the four-field model, this is an inconsistent result; in order to obtain (54), we assumed $x_\eta > 2\delta$ $(\nu_{ei}/\omega > 2m_i/m_e)$, but Eq. (55) requires $x_\eta < \delta_s$ $(\nu_{ei}/\omega < 1)$. Therefore, we conclude that (55) is not a physically relevant result.

Fortunately, using our results on the semi-collisional modes, we can easily find a dispersion relation for a collisionless $m = 1$ mode that is consistent with all our assumptions. In the collisionless regime, we have from (13) $x_{\eta_s}^2 = x_\eta^2 - i\delta_s^2 \simeq -i\delta_s^2$. Then substituting for x_{η_s} in Eq. (44) we obtain

$$(\omega - \omega_{*e})^3(\omega - \omega_{*i})^3 = (i\gamma_{less})^6 G(a)^2, \tag{56}$$

where the collisionless growth rate γ_{less} is

$$\gamma_{less} = \left(\frac{2}{\pi}\right)^{1/3} \left(\frac{m_i}{m_e}\right)^{1/3} k_\parallel' \, \delta_s \, c_s^{2/3}, \tag{57}$$

and $G(a)$ is given by Eq. (45). Using the definitions in Eq. (7), γ_{less} can be rewritten as

$$\gamma_{less} = \left\{\frac{T_e/T_i + 1}{\pi}\right\}^{1/3} k_\parallel' \, \delta_s \, \left(\frac{\rho_i}{\delta_s}\right)^{2/3}. \tag{58}$$

Once again, we believe we have obtained quite a remarkable result. Written in this form, γ_{less} differs from the collisionless growth rate found by Porcelli,[12] and also contained in Berk, Mahajan, and Zhang,[11] only by a factor of $2^{1/3}$. ($k_\parallel'$ appearing in our expression is absorbed into Porcelli's definition of ω_A.) Porcelli's analysis uses a fluid description for the electrons, with appropriate modifications of the Ohm's law, and a kinetic treatment of the ions valid for arbitrary value of the ion Larmor radius. Thus, the nearly exact agreement between our results and Porcelli's is one more example of how well the four-field model seems to describe the essential physics, despite its simplicity.

As in the previous section on the semi-collisional modes, the effects of ion sound waves in the collisionless regime can be found by asymptotically expanding $G(a)$ for large $a = i\Delta_e x_s/4\delta c_s \sim x_s/\rho_i$. Then the ion-sound-modified dispersion relation becomes

$$(\omega - \omega_{*e})^3(\omega - \omega_{*i})^3 = (i\gamma_{less})^6 \left\{1 + \left(\frac{\rho_i}{2}\right)^2 \left(\frac{T_e}{T_i} + 1\right) \frac{c_s^2 k_\parallel'^2}{(\omega - \omega_{*e})^2}\right\}. \tag{59}$$

A perturbative solution of (59) for $\omega \simeq i\gamma_{less} \gg \omega_*$ yields

$$\omega = \frac{\omega_{*e} + \omega_{*i}}{2} + i\gamma_{less} \left\{1 - \frac{1}{24}\left(\frac{T_e}{T_i} + 1\right) \rho_i^2 \frac{c_s^2 k_\parallel'^2}{\gamma_{less}^2}\right\}. \tag{60}$$

Again, the sound waves are found to be weakly stabilizing.

V. Discussion and Conclusions

We have analyzed the resistive branch ($\Delta' \to \infty$) of the $m = 1$ mode in collisional, semi-collisional, and collisionless regimes with a simplified four-field model of tokamak dynamics. The model includes some finite-Larmor radius effects (in the small FLR limit), parallel and perpendicular compressibility (we have used only the parallel compressibility feature here), and the electron and ion diamagnetic drift effects, with an isothermal equation of state. We showed that it reproduces very accurately a number of results obtained with more sophisticated kinetic treatments, e.g. the semi-collisional dispersion relation for $m = 1$ introduced by long-mean-free-path electron dynamics, and a related collisionless $m = 1$ mode made possible by finite electron inertia terms in the parallel Ohm's law.

We have also examined the effects of ion sound waves on the $m = 1$ mode and showed that the sound waves are weakly destabilizing in the collisional regime and stabilizing in the semi-collisional and collisionless regimes. However, for the modes that we have concentrated on with $\omega \simeq i\gamma \gg \omega_*$, the effect is weaker than it is for the $m \geq 2$ drift-tearing modes with $\omega \simeq \omega_{*e}$.

This work considers only linear modes in order to demonstrate the versatility and accuracy of the four-field model for high-temperature, low-collisionality regimes. The main usefulness of the model lies in nonlinear applications, where some of the modes discussed here will be studied nonlinearly, thus extending the previously performed purely resistive MHD calculations to regimes relevant for today's large tokamaks. Since both the semi-collisional and collisionless modes disccussed above are more robust and have larger growth rates than their purely resistive counterpart, the resistive $m = 1$ kink mode, a study of their nonlinear evolution may clarify some of the puzzling features of the tokamak sawtooth oscillations. Nonlinear numerical calculations with the four-field model will be the subject of a future publication.

Acknowledgements

Useful discussions with R. D. Hazeltine, P. J. Morrison, and M. Kotschenreuther on various versions of the four-field model, and with Y. Z. Zhang on FLR effects are greatfully acknowledged. Some of the algebraic manipulations were performed using *Mathematica*. This work was supported by the U.S. Department of Energy under contract No. DE-FG05-80ET-53088.

References

[1]S. von Goeler, W. Stodiek, and N. Sauthoff, Phys. Rev. Lett. **33**, 1201 (1974).

[2]B. B. Kadomtsev, Fiz. Plazmy **1**, 710 (1975) [Sov. J. Plasma Phys. **1**, 389 (1975)].

[3]B. Coppi, R. Galvao, R. Pellat, M. Rosenbluth, and P. Rutherford, Sov. J. Plasma Phys. **2**, 533, (1976) [Fiz. Plazmy **2**, 961 (1976)].

[4]G. Ara, B. Basu, B. Coppi, G. Laval, M. N. Rosenbluth, and B. V. Waddell, Ann. Phys. **112**, 443 (1978).

[5]M. N. Bussac, R. Pellat, D. Edery, and J. L. Soule, Phys. Rev. Lett. **35**, 1638 (1975).

[6]R. D. Hazeltine and H. R. Strauss, Phys. Fluids **21**, 1007 (1978).

[7]J. F. Drake, Phys. Fluids **21**, 1777 (1978).

[8]J. F. Drake, Y. C. Lee, L. Chen, P. H. Rutherford, P. K. Kaw, J. Y. Hsu, and C. S. Liu, Nucl. Fusion **18**, 1583 (1978).

[9]S. M. Mahajan, R. D. Hazeltine, H. R. Strauss, and D. W. Ross, Phys. Fluids **22**, 2147 (1979).

[10]F. Pegoraro, F. Porcelli, and T. J. Schep, Phys. Fluids B **1**, 364 (1989).

[11]H. L. Berk, S. M. Mahajan, and Y. Z. Zhang, Phys. Fluids B **3**, 351 (1991).

[12]F. Porcelli, Phys. Rev. Lett. **66**, 425 (1991).

[13]B. V. Waddell, M. N. Rosenbluth, D. A. Monticello, and R. B. White, Nucl. Fusion **16**, 3 (1976).

[14]R. E. Denton, J. F. Drake, R. G. Kleva, and D. A. Boyd, Phys. Rev. Lett. **56**, 2477 (1986).

[15]A. Y. Aydemir, Phys. Rev. Lett. **59**, 649 (1987).

[16]R. J. Hastie, T. C. Hender, B. A. Carreras, L. A. Charlton, and J. A. Holmes, Phys. Fluids **30**, 1756 (1987).

[17]J. A. Holmes, B. A. Carreras, L. A. Charlton, V. E. Lynch, R. J. Hastie, and T. C. Hender, Phys. Fluids **31**, 1202 (1988).

[18]A. Y. Aydemir, J. C. Wiley, and D. W. Ross, Phys. Fluids B **1**, 774 (1989).

[19]R. D. Hazeltine, C. T. Hsu, and P. J. Morrison, Phys. Fluids **30**, 3204 (1987).

[20]M. N. Bussac, D. Edery, R. Pellat, and J. L. Soule, Phys. Rev. Lett. **40**, 1500 (1978).

[21]R. D. Hazeltine and J. D. Meiss, Physics Reports **121**, 90 (1985).

[22]R. D. Hazeltine and D. W. Ross, Phys. Fluids **21**, 1140 (1978).

[23]A. Y. Aydemir, R. D. Hazeltine, J. D. Meiss, and M .Kotschenreuther, Phys. Fluids **30**, 4 (1987).

[24]J. F. Drake and Y. C. Lee, Phys. Fluids **20**, 1341 (1977).

[25]J. C. P. Miller, in *Handbook of Mathematical Functions*, edited by M. Abramowitz and I. A. Stegun (Dover, New York, 1968).

[26]T. S. Hahm, Ph.D Thesis, Princeton University, 1984.

[27]T. S. Hahm and L. Chen, Phys. Fluids **28**, 3061 (1985).

[28]Y. Z. Zhang, Bull. Am. Phys. Soc. **23**, 2074 (1988).

[29]B. Basu and B. Coppi, Phys. Fluids **24**, 465 (1981).

Figures

FIG. 1. Real frequency and the growth rate of the ion-sound-modified collisional $m = 1$ mode, calculated with an eigenvalue code that solves the linearized versions of Eqs. (1-4). a) The real frequency as a function of the square of the sound speed, $c_s^2 = \beta$. The solid line, the equation for which is given in the bottom of the figure, represents a best fit to the numerical data. b) The change in the growth rate, normalized to the resistive $m = 1$ growth rate, as a function of $c_s^2 = \beta$. Again, the solid line represents a best fit to the numerical data. The theory [Eq. (27)] predicts $\omega_r/\gamma_R = -3.33 \times 10^{-2}\beta$, and $(\gamma - \gamma_R)/\gamma_R = 3.33 \times 10^{-3}(-1 + \beta)$.

FIG. 2. The scaling of the growth rate of the semi-collisional $m = 1$ mode with resistivity η. The solid line, a best fit to the numerical data, gives $\gamma \sim \eta^{0.164}$, which should be compared with the theoretically expected $\eta^{1/7}$ scaling.

FIG. 3. The change in the growth rate of the semi-collisional $m = 1$ mode with $c_s^2 = \beta$, normalized to γ_{sc}, the semi-collisional growth rate without the ion-sound modifications.

FIG. 4. Eigenfunctions for the semi-collisional mode. a) $J_{||}$, b) $\mathcal{E}_{||}$. Locations of $r_s + x_{A*}$, $r_s + \rho_i$, and $r_s + x_s$, where r_s is the radius of the $q = 1$ surface, x_{A*} is the Alfvén layer-width, ρ_i is the ion Larmor radius, and x_s is the ion-sound layer width, are also shown.

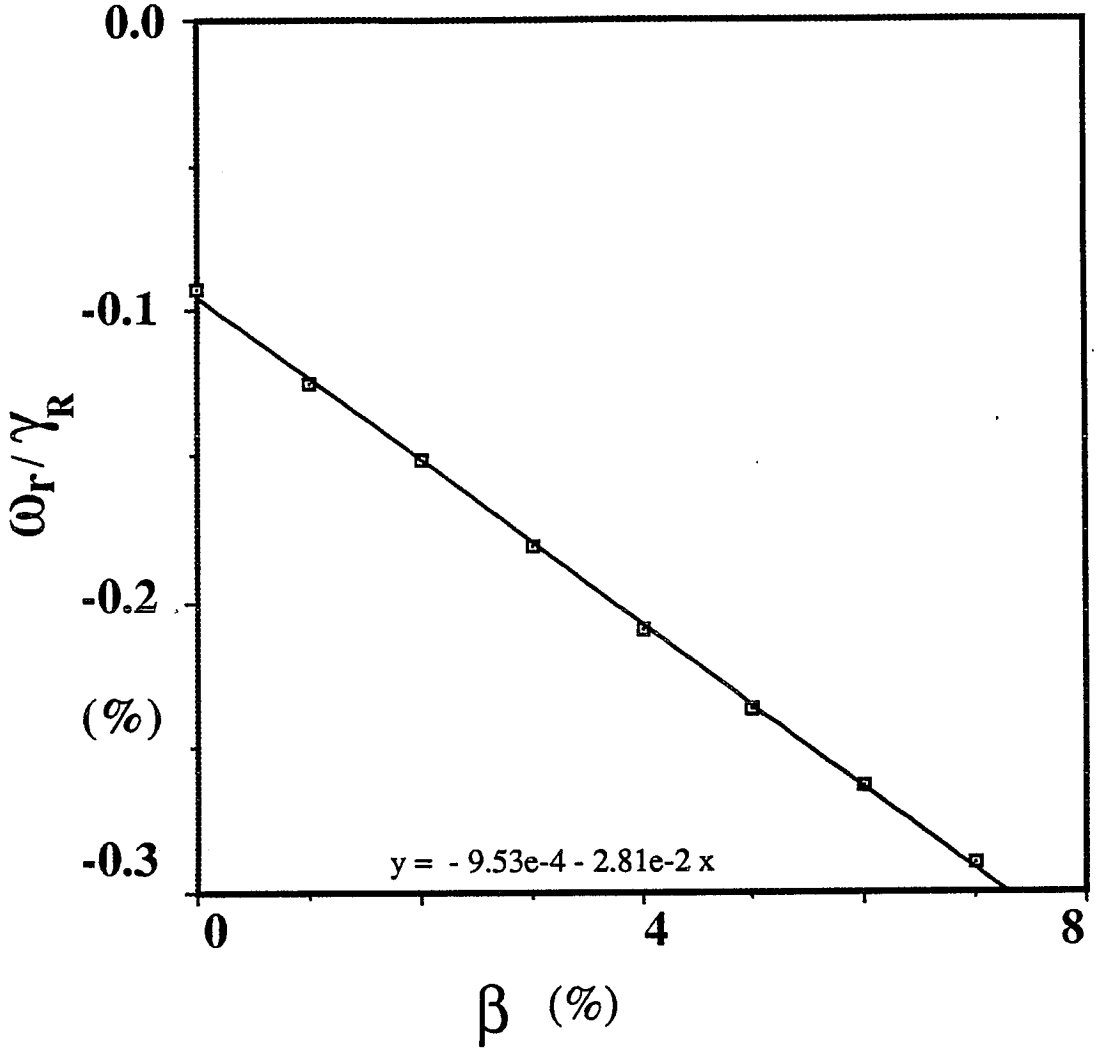

Fig. 1(a)

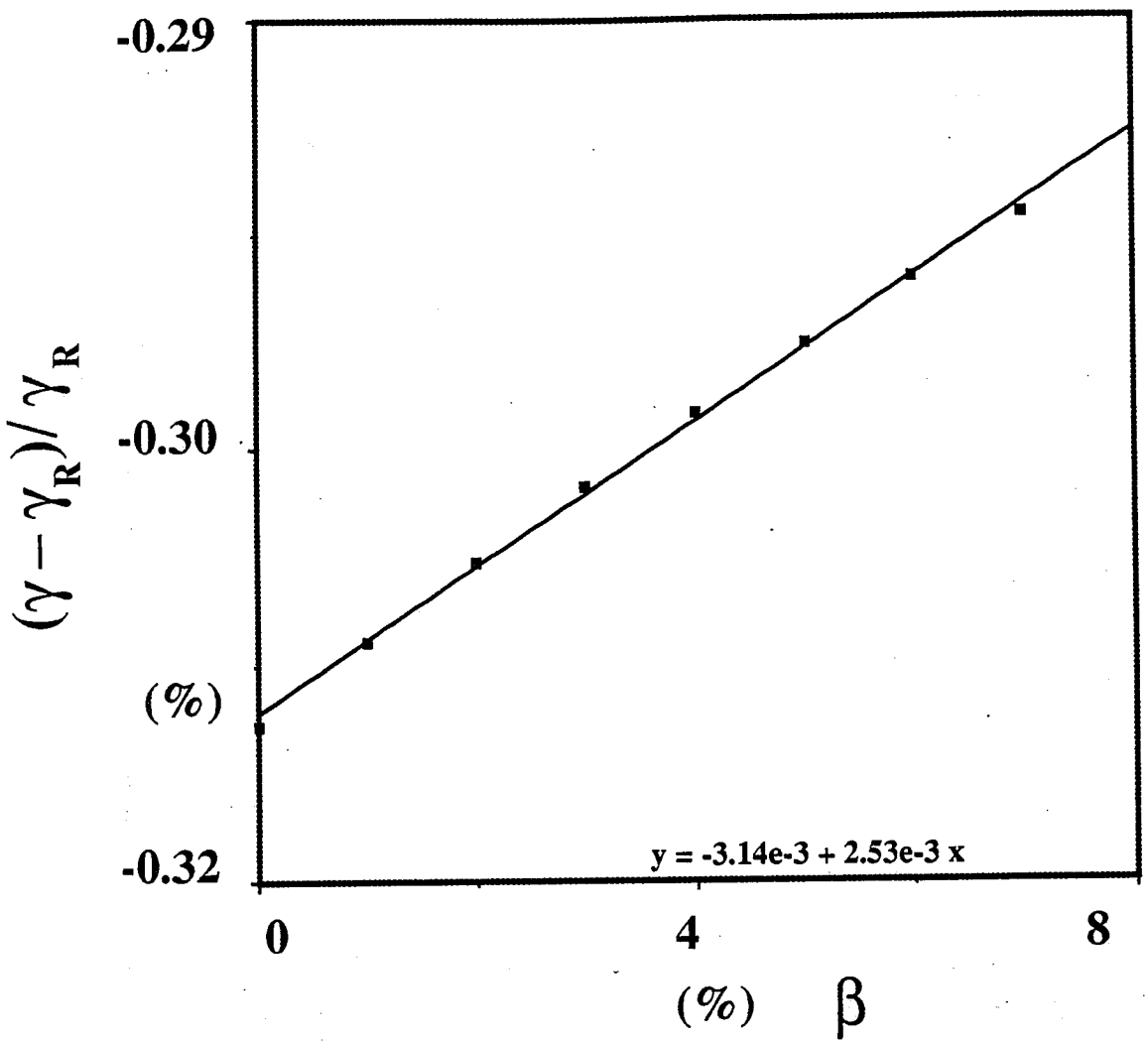

Fig. 1(b)

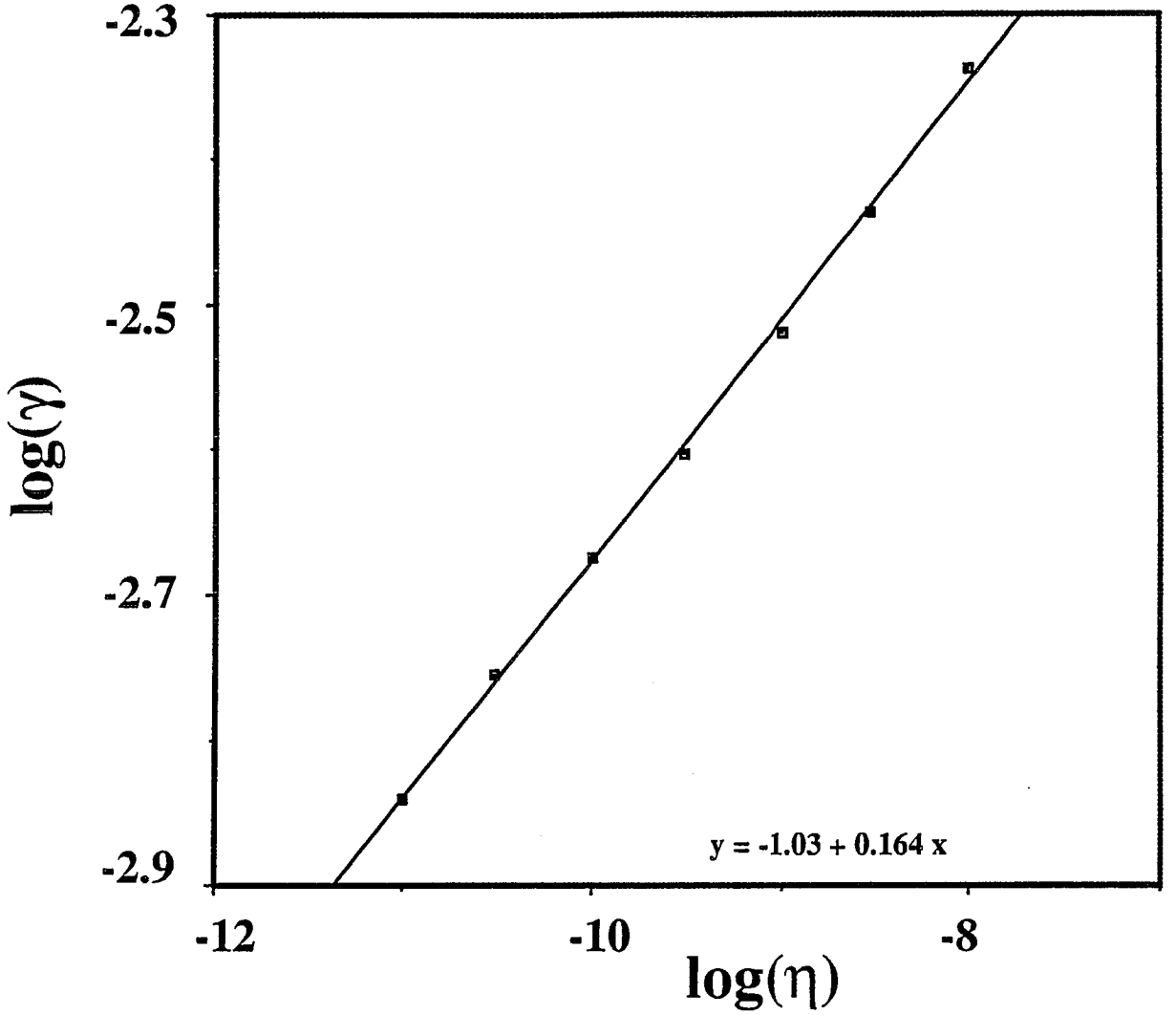

Fig. 2

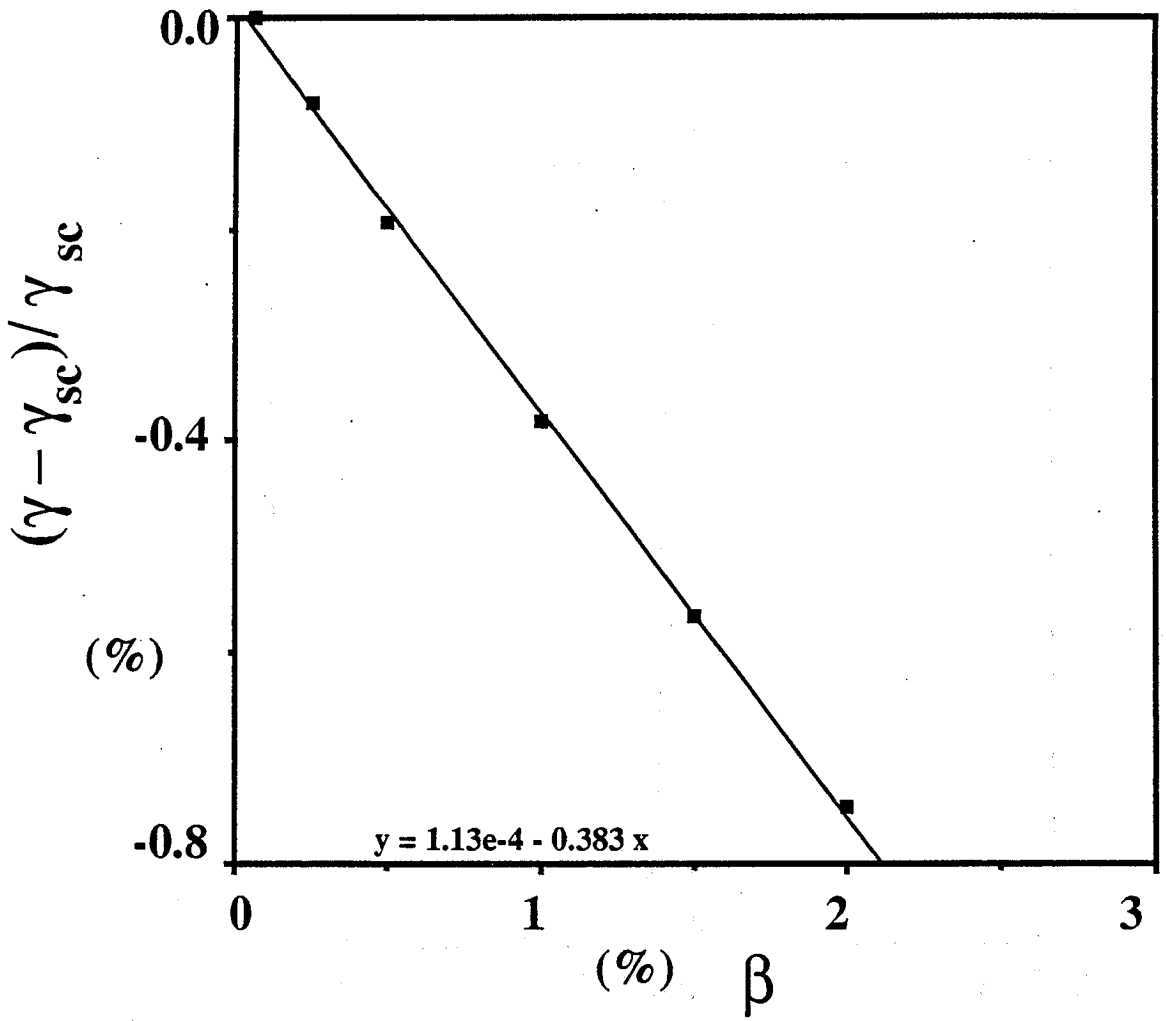

Fig. 3

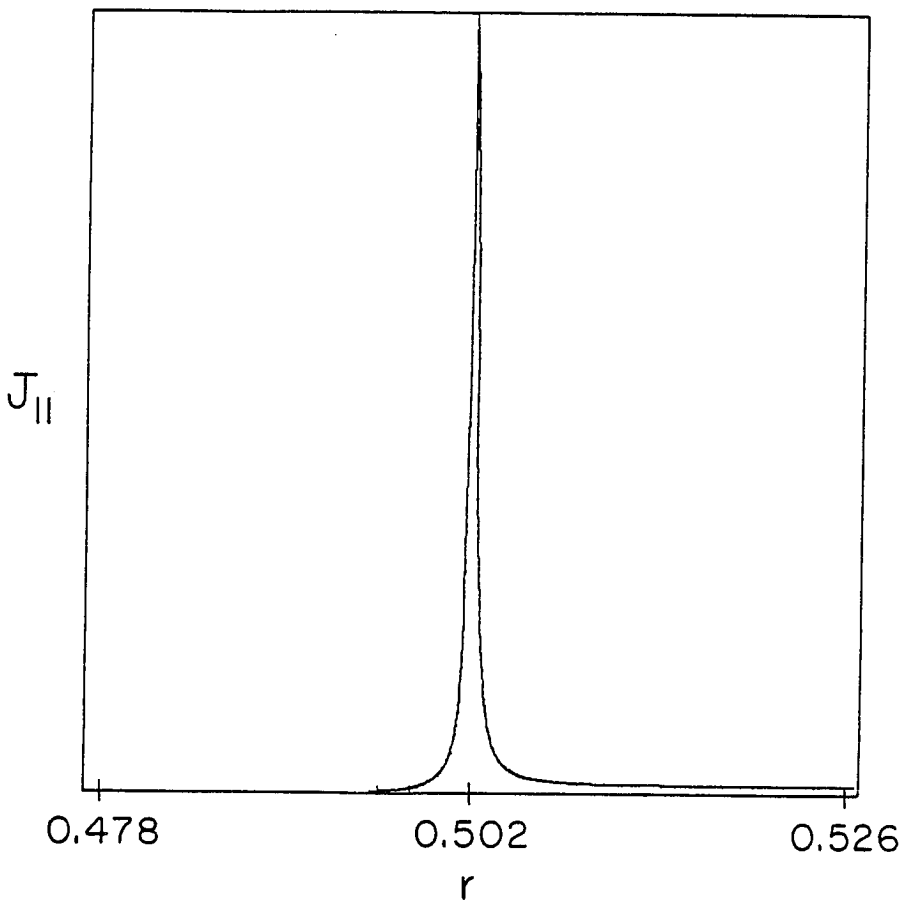

Fig. 4(a)

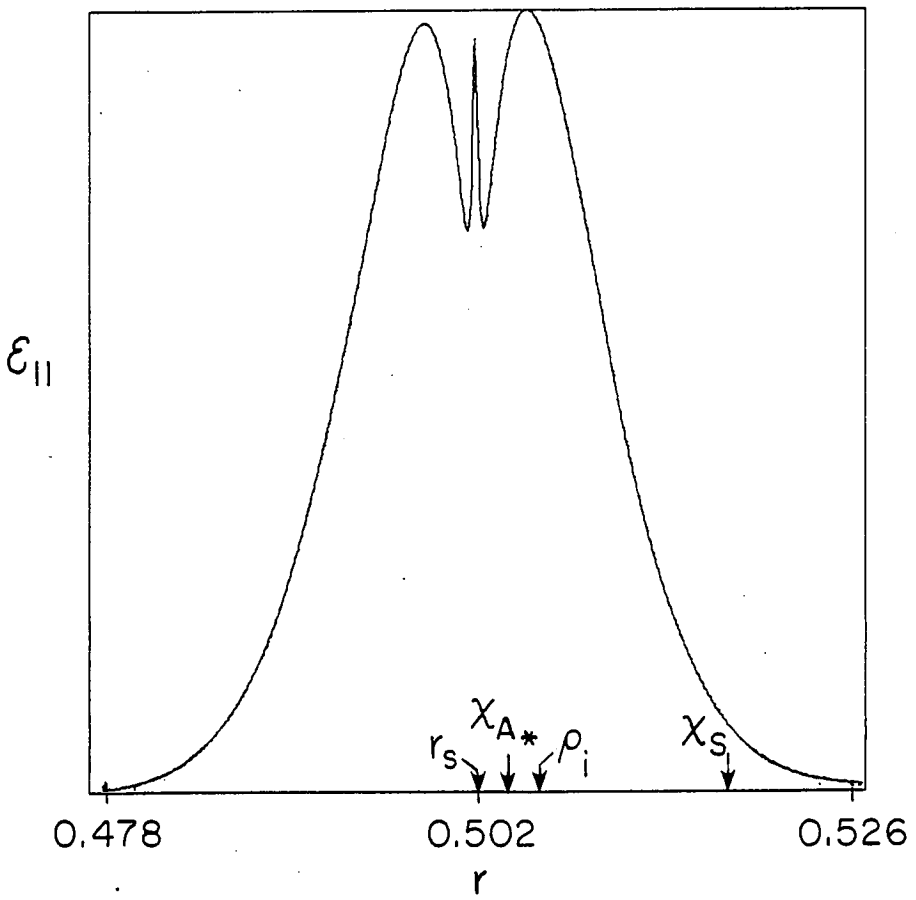

Fig. 4(b)